Title

X-Ray and Charged Particle Detection with CsI(Tl) Layer Coupled to a-Si:H Photodiode Layers

Authors

Fujieda, I.
Cho, G.
Drewery, J.
et al.

Publication Date

1990-10-01

LBL-29477

Lawrence Berkeley Laboratory
UNIVERSITY OF CALIFORNIA

Physics Division

Presented at the IEEE Symposium on Nuclear Science,
Washington, DC, October 19–23, 1990, and to be
published in the Proceedings

X-Ray and Charged Particle Detection with CsI(Tl) Layer Coupled to a-Si:H Photodiode Layers

I. Fujieda, G. Cho, J. Drewery, T. Gee, T. Jing, S.N. Kaplan,
V. Perez-Mendez, D. Wildermuth, and R.A. Street

October 1990

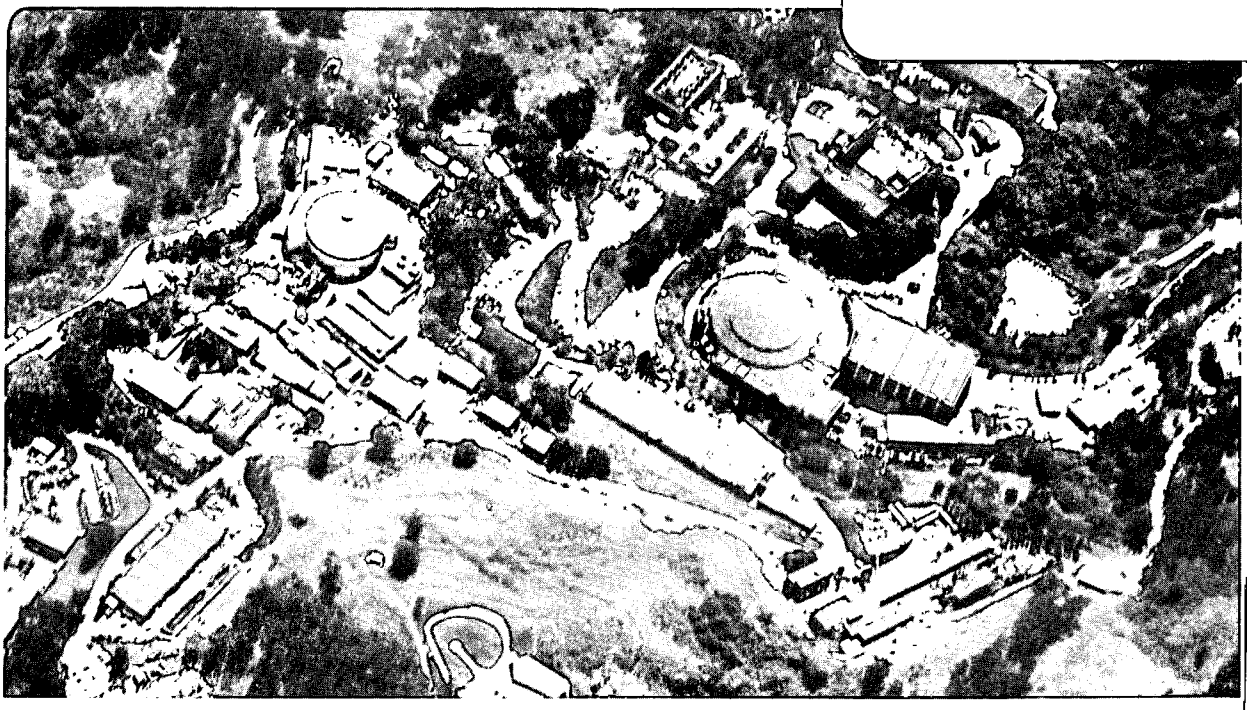

Prepared for the U.S. Department of Energy under Contract Number DE-AC03-76SF00098.

DISCLAIMER

X-ray and Charged Particle Detection with CsI(Tl) Layer Coupled to a-Si:H Photodiode Layers

I. Fujieda, G. Cho, J. Drewery, T. Gee, T. Jing, S.N. Kaplan, V. Perez-Mendez, D. Wildermuth
Lawrence Berkeley Laboratory, 1 Cyclotron Rd. Berkeley, CA 94720
R.A. Street
Xerox Palo Alto Research Center, 3333 Coyote Hill Rd. Palo Alto, CA 94304

Abstract

A compact real-time X-ray and charged particle imager with digitized position output can be built either by coupling a fast scintillator to a photodiode array or by forming one on a photodiode array directly. CsI(Tl) layers 100-1000 μm thick were evaporated on glass substrates from a crystal CsI(Tl). When coupled to a crystalline Si or amorphous silicon (a-Si:H) photodiode and exposed to calibrated X-ray pulses, their light yields and speed were found to be comparable to those of a crystal CsI(Tl). Single β particle detection was demonstrated with this combination. The light spread inside evaporated CsI(Tl) was suppressed by its columnar structure. Scintillation detection gives much larger signals than direct X-ray detection due to the increased energy deposition in the detector material. Fabrication of monolithic type X-ray sensors consisting of CsI + a-Si:H photodiodes is discussed.

I. INTRODUCTION

a-Si:H has been investigated as a possible alternative for radiation detector material for high energy physics experiments, medical imaging, material and life science studies [1,2,3]. Early efforts to make X-ray detectors with a-Si:H by Wei et al. [4] used a phosphor such as $CdWO_4$ and ZnS(Ni). Mochiki et al. [5] used a facsimile head to detect X-ray fluences with a good spatial resolution. Recently, Ito et al. fabricated a monolithic type X-ray sensor by depositing a-Si:H layers directly on a ceramic scintillator Gd_2O_2S:Pr:Ce:F and reported that the light yield of their ceramic scintillator is comparable to CsI(Tl) and that its scintillation decays to 1/10 of the initial level in 5 μs [6]. Street et al. obtained X-ray images with a two-dimensional a-Si:H photodiode array coupled to a Lanex (Kodak) intensifying screen for X-ray films (Gd_2O_2S:Tb) [7]. a-Si:H photodiodes 1-2 μm thick coupled to Lanex have been shown to give a 100-330 times larger signal size for detecting X-rays used in medical imaging compared to the a-Si:H diode alone [7,8].

This work was supported by the Director, Office of Energy Research, Office of High Energy and Nuclear Physics, Division of High Energy Physics, and Office of Health and Environmental Research, Division of Physics and Technological Research of the U.S. Department of Energy under contract No. DE-AC03-76SF00098.

Choice of a scintillator is dependent on specific requirements for each detector application, namely, the type of radiation, speed requirement and spatial resolution in case of imaging applications. For most imaging applications, however, a fast bright scintillator with some built-in light guiding structure is desirable since the light spread inside a scintillator degrades the spatial resolution of a position-sensitive detector. Vacuum evaporated CsI forms columns parallel to the evaporation direction, confining the light to produce a sharper image output [9,10]. CsI(Na) is used for image intensifier application due to its good emission spectrum matching to the photocathode sensitivity. For coupling to photodiodes, CsI(Tl) has the following advantages over CsI(Na); (a) better emission spectrum matching to a photodiode quantum efficiency [11], (b) larger light yield [12] and (c) better stability in air. It has the disadvantage of a slightly slower scintillation decay. Emission spectra are shown in Fig.1 for CsI(Na) and CsI(Tl) together with quantum efficiencies of an a-Si:H photodiode [6] and S-11 photocathode (Sb-Cs) [13].

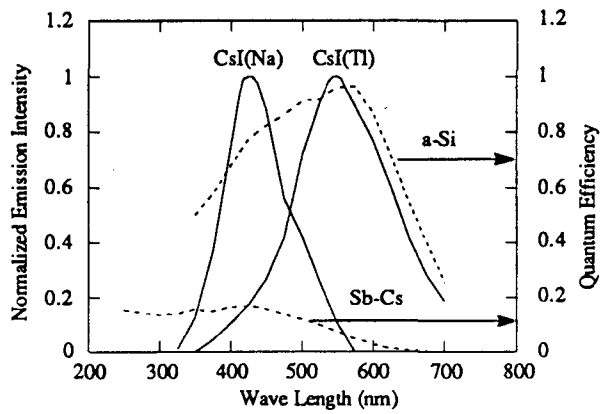

Fig.1 Normalized emission spectra of CsI(Na) and CsI(Tl) and quantum efficiency of an a-Si:H photodiode and a photocathode.

The evaporation process and measurements on properties of evaporated CsI(Tl) layers such as signal yield, speed, light spread and radiation damage are described in the next section. Detection of X-ray pulses and single β particles with an evaporated CsI layer coupled to a photodiode is demonstrated.

A monolithic detector construction and its use to detect X-ray pulses is discussed in the following sections.

II. CsI EVAPORATION AND LIGHT YIELD OPTIMIZATION

A. CsI evaporation

The vacuum evaporation setup used at LBL is shown schematically in Fig.2. The important parameters are the substrate temperature and the boat temperature. The higher substrate temperature tends to give larger fiber structure and better adhesion to smooth glass surfaces. Lower substrate temperature tends to give finer columnar structure. The boat temperature determines the evaporation rate. The glass surface should be roughened to improve CsI adhesion when used as a low temperature substrate (≤~300°C).

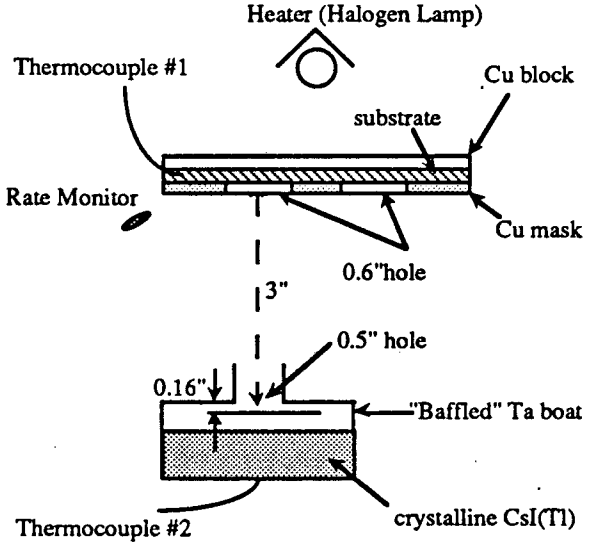

Fig.2 The vacuum evaporation setup for CsI faceplate fabrication.

CsI(Tl) layers 100-1000 μm thick were evaporated from single crystal CsI(Tl) chips supplied by Engelhard Corp. The glass substrate was initially heated at 100 °C but its temperature increases up to 140 °C at the end of a run due to radiation heating from the Ta boat. The evaporation rates were varied to improve the light yield.

B. CsI signal yield

Evaporated CsI(Tl) layers and single crystal CsI(Tl) samples were exposed to calibrated 1-2 μs 50 kV_p X-ray pulses through a 1.25 mm-diameter hole. A crystalline silicon photodiode with 1x1 cm^2 area (Hamamatsu S1723-04) [13] was coupled to these evaporated CsI(Tl) layers as well as to encapsulated crystal CsI(Tl) in Al housings made by Bicron. The Hamamatsu photodiode has been used extensively because its quantum efficiency is well characterized by the manufacturer although that of an a-Si:H photodiode can be made equally good or better. A thin Al sheet covered the top surface of the evaporated layers to reflect back the scintillation light. A charge-sensitive preamplifier (Tennelec TC170) and a quasi-Gaussian shaping amplifier with 9 μs peaking time were used to measure the charge produced in the photodiode. The signal was expressed in terms of number of electron-hole pairs produced when absorbing X-ray energy equivalent to 1 MeV. The results are summarized in Fig.3.

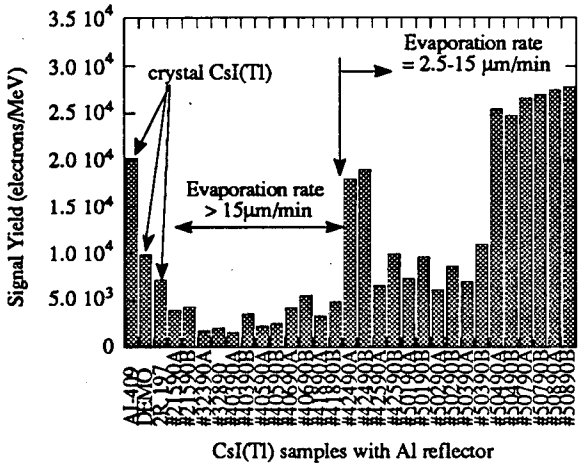

Fig. 3 Signal yields from a number of evaporated CsI(Tl) layers (their ID #'s are also production dates in most cases) as well as three crystal CsI(Tl) samples.

The first three (AI-409, DEMO, 2R.197) are all crystal CsI(Tl) made by Bicron. AI-409 is a 5 mm thick 5 mm diameter cylinder of CsI(Tl). 2R.197 is a 5 mm thick 5 cm diameter disk of CsI(Tl). DEMO has the same dimensions as 2R.197 but its 5 mm thick CsI(Tl) disk was cut by a wire-saw into 2 mm x 2 mm columns and the gaps between columns were filled with reflector materials. It is possible that the lateral light spread inside the crystal resulted in the smaller signal size for DEMO and 2R.197. Among the evaporated CsI(Tl) layers, the first twelve samples were evaporated at a rate faster than 15 μm/min. The last sixteen samples were evaporated at a well-controlled constant rate (about 2.5-15 μm/min). Samples labeled as "A" were centered against the boat and were two to three times thicker than the ones labeled as "B", which were off-centered. The evaporation rate was calculated from the evaporation time and the thickness of the "A" sample. The signal size for these layers was increased by as much as about 50% by putting a thin aluminanized mylar sheet as a reflector on top of the CsI(Tl) layers.

C. CsI signal yield optimization

The light yield of CsI(Tl) is sensitive to the evaporation conditions, especially the boat temperature which determines the evaporation rate. CsI(Tl) layers 230-460 μm thick were evaporated at different boat temperature, and hence different evaporation rates and signal yields were obtained with the 50kV_p X-ray. The results are shown in Fig.4. With the optimum preparation, the light yield of evaporated CsI(Tl) layers can be made close to a single crystal CsI(Tl) as demonstrated by samples made at later time.

The Tl concentration is known to affect the signal yield in crystalline CsI(Tl) coupled to a photodiode [14]. The Tl concentrations in our evaporated layers were evaluated by X-ray Reflection Fluorescence analysis (XRF) [15] and plotted against their signal yields from the 50 kV_p X-ray measured before. The results are shown in Fig.5. The same behavior is seen for our evaporated layers and the crystalline CsI(Tl) in ref.[14]. It is confirmed that the layers evaporated at a slower rate contains more Tl than those made at a faster rate. The XRF measurements showed that the evaporated layer had Tl concentration up to 20-30% less than the source CsI(Tl) crystal.

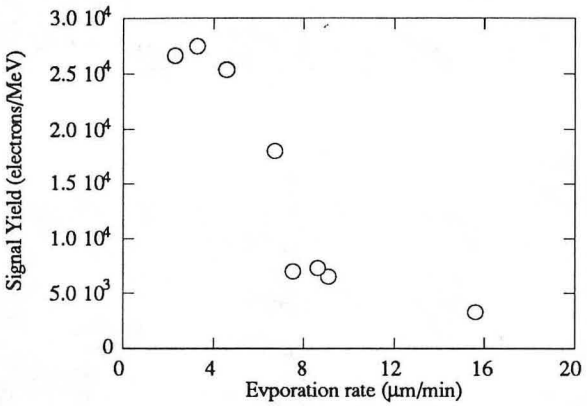

Fig. 4 Signal yields from CsI(Tl) evaporated at different rates. The rate is based on the samples labeled as A which were centered against the boat.

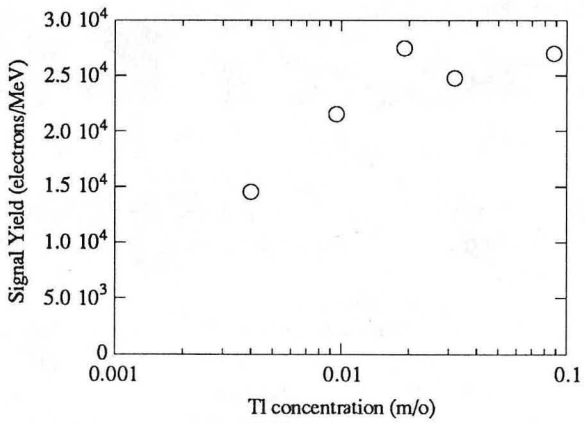

Fig.5 Signal yields from CsI(Tl) with different Tl concentrations as measured by XRF.

III. CHARACTERISTICS OF EVAPORATED CsI(Tl)

A. speed and signal yield

The decay constant of a scintillator can be obtained by analyzing the charge-sensitive preamplifier output when the scintillator coupled to a photodiode is irradiated by a short X-ray pulse. The following experiment and analysis were conducted to compare the speed and signal yields of our evaporated CsI(Tl) layers to those of Gd_2O_2S screens.

Various scintillators (the Gd_2O_2S:PrCeF supplied by Hitachi Metal, Lanex made by Kodak and a CsI(Tl) layer evaporated at LBL) were placed on top of the Hamamatsu photodiode (S1723-04) and were exposed to 1.4 μs wide 50 kV_p X-ray pulses. The charge-sensitive preamplifier outputs was fed directly into a digital storage oscilloscope (Tektronix 2430) and the digitized wave forms were analyzed by a computer. A detailed analysis is given in the Appendix.

First, the Hitachi scintillator 1.1 mm thick and our evaporated CsI(Tl) 461 μm thick were compared as shown in Fig.6 together with the signal from the crystalline Si diode (S1723-04) alone. Both scintillators absorbed all the X-ray energy. The linear portion of the c-Si signal extends about 1.2 μs, confirming the duration of a constant X-ray intensity. The asymptotic levels for these scintillators agree roughly and are equivalent to 2.5×10^4 electrons/MeV. The analysis in the Appendix on our measurements shows that the decay constants of these scintillators are 1.1 μs for the CsI(Tl) and 3.5 μs for the Hitachi layer.

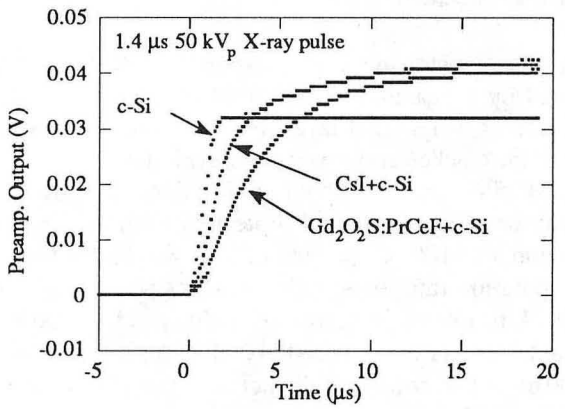

Fig.6 Preamplifier output for the CsI(Tl) layer and the Hitachi screen.

Second, Lanex and our CsI(Tl) layer were compared. The Lanex screen was about 300 μm thick and mounted on a thin plastic plate. The CsI(Tl) was 315 μm thick and was evaporated on 1 mm thick glass. Unless a scintillator absorbs all the X-ray energy, the signal contains a contribution from direct electron-hole pair creation in the photodiode by the penetrating X-rays. This is the case for the 300 μm thick Lanex screen and the direct signal contribution was measured by placing a thin opaque sheet between a scintillator and S1723-04. The resultant wave forms were subtracted from the wave forms observed without the opaque sheet. The average energy of the X-ray was 30 keV and the direct contribution was about 20% of the total charge collected by the photodiode in

the case of the Lanex screen and 10% for the CsI(Tl) layer. The wave forms after subtraction of the direct contributions are shown in Fig.7. The RC decay constant is about 1.06 ms The Lanex signal shows a peak and then decays more slowly than the CsI signal. The analysis in the Appendix shows that the decay constant of Lanex is 0.48 ms and that the total signal yield is comparable to that of the CsI(Tl) layer.

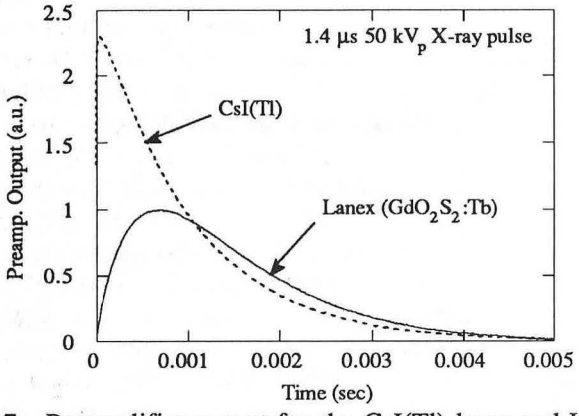

Fig.7 Preamplifier output for the CsI(Tl) layer and Lanex. Both curves were normalized against the peak value of the Lanex data.

B. Spatial resolution

The columnar structure of the evaporated CsI(Tl) layers was confirmed by a Scanning Electron Micrograph (SEM). A small piece of evaporated layer material was cut by a razor blade and the cracked surfaces were observed by a SEM. The two SEM photographs shown in Fig.8 clearly show the columnar structure. The substrate temperature during the evaporation was 100 °C for Fig.8(a) and 200 °C for Fig.8(b). The evaporation rate for the 100 °C layer was the optimum ones (< 4 μm/min) in terms of light yield. Only the substrate temperature was raised to 200 °C for the layer shown in Fig.8(b). The columnar diameter of the 100 °C layer is about 10 μm whereas that of the 200 °C layer is about 15-20 μm. The light yield of the 200 °C layer was almost the same as the 100 °C layer.

Next, the light spread inside evaporated CsI(Tl) layers as well as the Hitachi scintillator (Gd_2O_2S:PrCeF) and the Lanex screen (Gd_2O_2S:Tb) were characterized using a narrow beam of He-Ne Laser light (633 nm) and a facsimile head as a position sensitive light detector. The facsimile head module made by SEIKO-EPSON (a linear a-Si:H photodiode array with a TFT attached to each photodiode) had 400 dpi (dots-per-inch) resolution [16]. The external circuit was the standard readout electronics designed for the facsimile application and it gave a sequence of voltage pulses, each pulse height corresponding to a charge produced by each photodiode element. This pulse sequence was digitized and stored by a Tektronix 2430 oscilloscope and data were transfered to a computer for

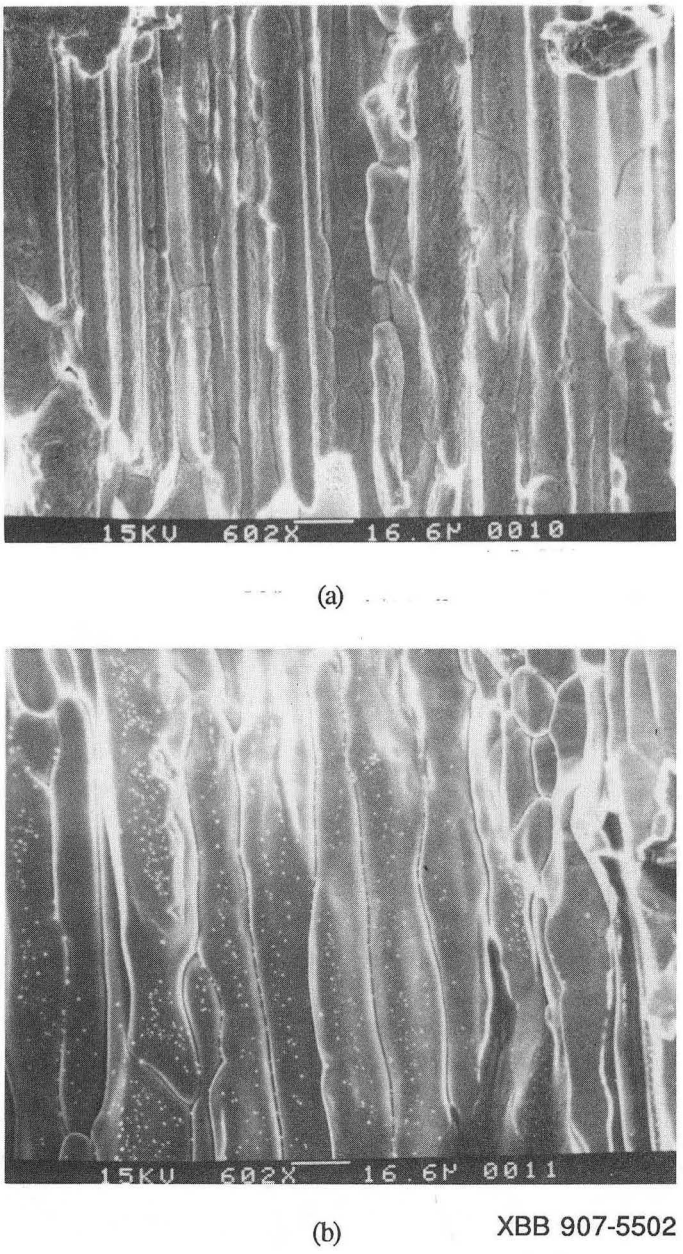

Fig.8 SEM photograph of cracked surfaces of CsI(Tl) layers evaporated at substrate temperature of 100 °C (a) and 200 °C (b).

analysis. First, the photodiode array was exposed to a parallel light beam from the Laser through a narrow slit without a scintillator between the slit and the array. The slit opening was set to 50 μm so that only one pixel of the 1D-photodiode array gave a signal. The position of the array was adjusted such that the signal was maximum. Second, a scintillator (either a 425 μm or 894 μm thick evaporated CsI(Tl) layer or one of the two Gd_2O_2S compounds) was placed on the photodiode array and the same light beam was used to expose the scintillator. A line spread function for each scintillator was obtained from the pulse sequence when the time was converted into position. The 425 μm and 894 μm thick CsI(Tl) layer used in this experiment were evaporated on

roughened glass substrates with the optimized parameters and were peeled from the substrates. The Hitachi scintillator (Gd_2O_2S:PrCeF) was 1.1 mm thick and the Lanex screen (Gd_2O_2S:Tb) was 300 μm thick.

The line spread function normalized for each scintillator is shown in Fig.9 and Fig.10. Spatial resolution is often expressed in terms of a full width at half maximum (FWHM) of a line spread function. The resolution of both of the 425 μm and 894 μm thick evaporated CsI(Tl) layers is ≈ 200 μm FWHM, whereas those of the Gd_2O_2S compounds are ≈ 400 μm for the 300 μm thick Lanex screen and ≈ 1 mm for the 1.1 mm thick Hitachi scintillator. This is not a clean quantitative comparison because the thickness of each scintillator is not the same, but it indicates that the light spread inside the evaporated CsI)Tl) layer is suppressed by its columnar structure.

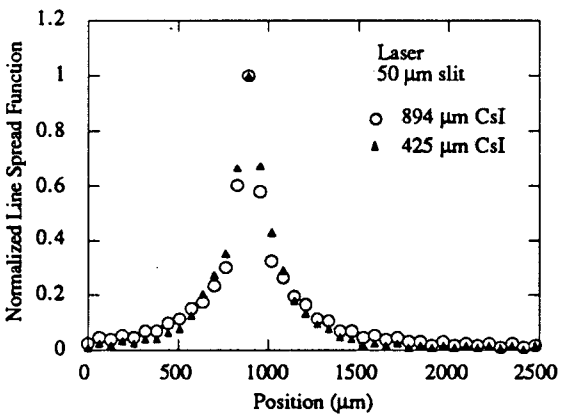

Fig.9 Line spread functions for CsI(Tl) layers obtained with the Laser light beam.

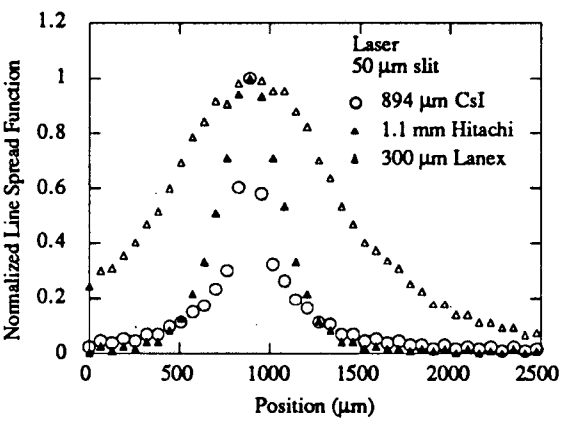

Fig.10 Line spread functions for the CsI(Tl) and the two Gd_2O_2S compounds obtained with the Laser light beam.

A similar experiment was conducted with X-ray beam instead of the laser. The 425 μm thick CsI(Tl) layer coupled to the linear a-Si:H photodiode array was exposed to 50 kV_p X-ray (DC) through a 75 μm tungsten slit. Due to the small X-ray signal size compared with the ripples of output pulses from the readout electronics designed for facsimile, the output pulse sequence without the X-ray exposure was recorded separately and was subtracted from the X-ray output pulse sequence to obtain a line spread function shown in Fig.11.

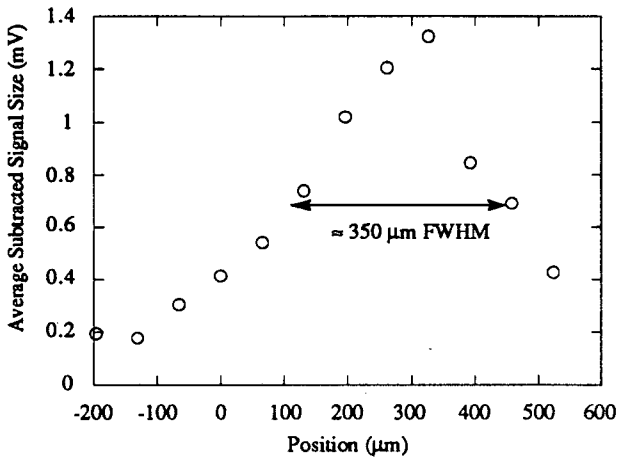

Fig.11 Line spread functions for the CsI(Tl) obtained with X-ray. For detail, see the text.

The discrepancy between the Laser measurements and the X-ray measurement is due to the fact that the scintillation light is emitted isotropically. Total reflection occurs on the columnar surface if the incident angle of the light is larger than the critical angle. This is calculated to be 34° for the CsI and air boundary [17]. Some of the scintillation light is trapped inside the scintillator by internal reflection. Most of the light (83%) [17] come out from the CsI layer by successive reflection but the directions of these light at the end of the columns can be as much as 34° apart from the column direction of the CsI layer. On the other hand, the Laser light is incident on the scintillator normally and a large angle scattering on the columnar surface is unlikely, leading to a narrower light spread.

C. Radiation damage

An evaporated CsI(Tl) layer 125 μm thick was exposed to γ rays from a Co-60 source at the irradiation facility at LBL. The nominal activity of the Co-60 source was 6000 Ci. The CsI(Tl) sample was placed at 10-30 cm away from the source and left for various time periods as required for the total dose. The signal size was measured with and without a reflector after each exposure and plotted in Fig.12. Also shown in the figure are the data for 1 cm thick crystal CsI(Tl) taken from ref.[18]. Each signal amplitude is normalized against its zero dose level.

The dose required to reduce the signal size by a factor of 2 for the thin evaporated layer is about 50 times larger than that for the 1 cm crystal sample. The signal loss is systematically larger when the light collection is improved by the reflector. This suggests that the radiation damage changed transmission

properties of the scintillator, in agreement with more detailed studies on crystal CsI(Tl) [18].

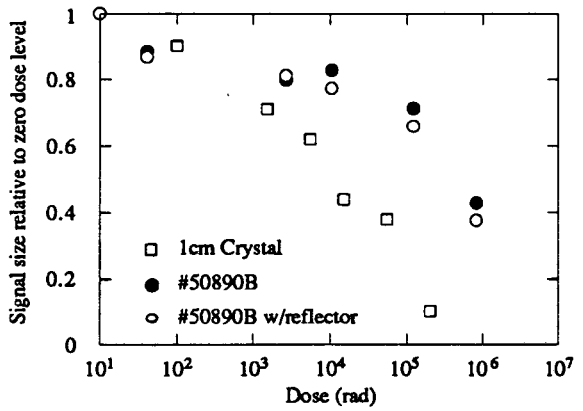

Fig.12 Light yield decrease due to radiation damage for a thin CsI(Tl) layer.

IV. X-RAY AND β PARTICLE DETECTION

A. X-ray detection

The detection of X-ray pulses was demonstrated with a 10 μm a-Si:H p-i-n diode and a 233 μm thick CsI(Tl) layer. The open circles in Fig.13 show the pulse height spectrum for direct X-ray detection when a 10 μm thick, 3 x 3 mm^2 area a-Si:H p-i-n diode was reverse-biased at 100 V and exposed to the 50 kV_p X-ray pulses directly. The structure of the diode was 0.8 mm glass / SnO_2 / 30 nm-p+ / 10 μm-i / 30 nm-n+ / Cr. Next the glass side of this diode was coupled to the glass substrate of a 233 μm thick CsI(Tl) layer. The pulse height spectrum of the signal for the same X-ray exposure is shown by solid circles in Fig.13.

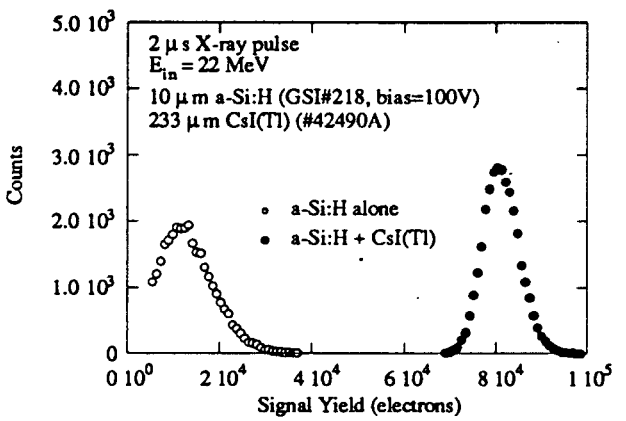

Fig.13 Detection of X-ray by a 10 μm thick a-Si:H diode with and without a 233 μm thick CsI(Tl).

The direct signal size of about $1.2x10^{+4}$ electrons is consistent to what we expect from W (the average energy to create an electron-hole pair) of ≈ 5 eV [1]. As for the scintillation signal size, it is about 25 % of what is expected from the layer used. This loss is accounted mostly by the inadequate light collection by the a-Si:H diode.

B. β particle detection

Evaporated CsI(Tl) layers 315 μm, 461 μm and 894 μm thick were coupled to the Hamamatsu photodiode S1723-04. This photodiode was used since its small capacitance reduces the noise level from the charge-sensitive amplifier. A thin Al reflector was put on the scintillator for better light collection. This assembly was exposed to β particles from a Bi-207 source. The output of the photodiode was amplified by the charge-sensitive preamplifier and shaped by a quasi-Gaussian shaping amplifier (6.4 μs peaking time). The resultant pulse height spectrum is shown in Fig.14. The solid and open circles and solid triangles in Fig.14 show the spectra obtained with a 315 μm, 461 μm and 894 μm thick CsI(Tl), respectively. The open triangles show the spectrum when the source was out.

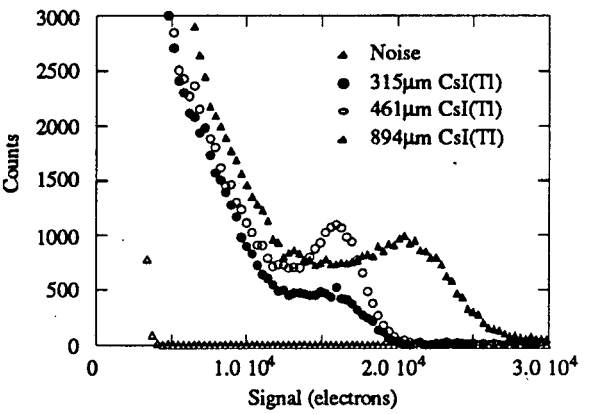

Fig.14 Detection of β particles from a Bi-207 source by an evaporated CsI(Tl) layer coupled to a photodiode.

The monoenergetic β particles from the Bi-207 source create a peak only with the thicker CsI(Tl) layers and there is a significant amount of counts in low energy tail for the both scintillators. This suggests that the a large number of electrons escape from the scintillator. When the layer thickness is comparable to the range of electron, some electrons deposit their full energy, creating a peak in a pulse height spectrum [19]. Nevertheless, single β particles can be detected by this detector assemble well above the noise. High energy minimum ionizing particles will produce ≈ 10,000 e-h pairs for a 500 μm thick CsI(Tl) layer coupled to a 70% quantum efficiency photodiode and the signal to noise ratio will be larger than 10.

V. MONOLITHIC CHARGED PARTICLE AND X-RAY DETECTOR

The scintillator materials were coupled to a photodiode through a glass or a transparent plastic plate in all the cases discussed so far. However, it is advantageous to have CsI evaporated directly on an a-Si:H photodiode for better optical coupling between the two [20]. The structure of the monolithic X-ray sensor is shown schematically in Fig.15. The purpose of the polyimide layer is to improve CsI adhesion to the transparent conductive layer ITO.

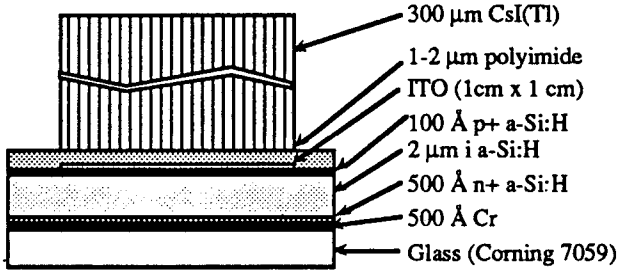

Fig.15 Monolithic X-ray sensor consisting of CsI(Tl) and a-Si:H photodiode.

A prototype for this structure was fabricated and exposed to the calibrated X-ray pulse. The pulse height analysis is shown in Fig.16. Due to the large area and hence the large capacitance of this a-Si:H photodiode (≈ 5,000 pF), the noise was about 50,000 electrons (FWHM), which is the expected value for the charge-sensitive preamplifier.

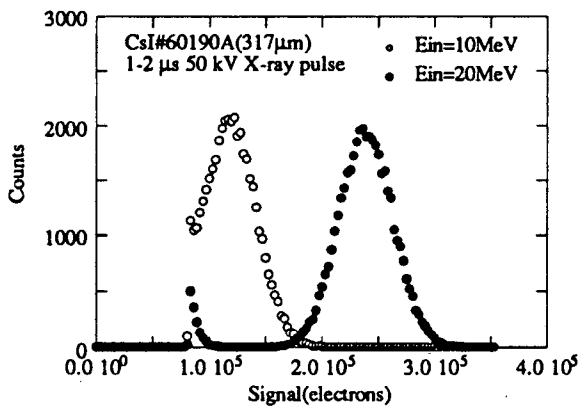

Fig.16 X-ray pulse height analysis for the monolithic X-ray sensor consisting of CsI(Tl) and a-Si:H photodiode.

VI. CONCLUSION

CsI(Tl) layers 100-900 μm thick were evaporated from crystal CsI(Tl) chips on glass substrates as well as on a-Si:H layers. They were found to give light yields and speed comparable to crystal CsI(Tl). Concentration of Tl atoms in the evaporated layers was measured and correlated with the light yield. The light spread inside the scintillator was suppressed by the columnar structure of the evaporated CsI(Tl) layers. This type of CsI(Tl) X-ray converter layer makes it possible to make digital radiography detectors with a spatial resolution ≈ 350 μm FWHM when coupled to the matrix a-Si:H photodiode arrays made at Xerox PARC [7]. A monolithic type X-ray sensor consisting of CsI(Tl) and a-Si:H photodiodes was fabricated. Further improvement in signal amplitude for this device is possible by optimizing the photodiode performance as well as the optical collection efficiency.

ACKNOWLEDGEMENT

We thank Drs. R. Weisfield and C.C. Tsai of Xerox Palo Alto Research Center for making some of the a-Si:H samples. We are also grateful to Dr. D. Johnson of Varian Corp. and Dr. B. Utts of Engelhard Corp. for their valuable comments about the CsI evaporation process and Drs. D. Hammond and C. Borlinghaus of Engelhard Corp. for supplying crystal CsI(Tl). Our appreciations are extended to Dr. Y. Tsukuda of Hitachi Metal Inc. and Dr. J. Price of Bicron for sending sample scintillators. We are indebted to Dr. R.D. Giauque of Lawrence Berkeley Laboratory for the XRF analysis.

REFERENCES

[1] V. Perez-Mendez, G. Cho, J. Drewery, I. Fujieda, S. N. Kaplan, S. Qureshi and R. A. Street, "Properties and Applications of Amorphous Silicon in Charged Particle, Gamma Ray and Light Detection," LBL-28339 (February 1990). To be published as a chapter in *Physics and Applications of Amorphous and Microcrystalline Semiconductor Devices*, Edited by J. Kanicki, Artech House, Boston, MA, Fall 1990.

[2] V. Perez-Mendez, G. Cho, I. Fujieda, S. N. Kaplan, S. Qureshi and R. A. Street, "The Application of Thick Hydrogenated Amorphous Silicon Layers to Charged Particle and X-Ray Detection," LBL-26998 (April 1989), *MRS Society Proceeding*, vol.149, pp.621-630, 1989.

[3] I. Fujieda, G. Cho, S. N. Kaplan, V. Perez-Mendez, S. Qureshi and R. A. Street, "Applications of a-Si:H Radiation Detectors," LBL-27457 (July 1989), *J. Non-Crystalline Solids*. vol. 115, pp.174-176, 1989.

[4] Wei Guang-Pu, H. Okamoto and Y. Hamakawa, "Amorphous-Silicon Photovoltaic X-Ray Sensor," *Jpn. J. Appl. Phys.* vol. 24, pp. 1105-1106, 1985.

[5] K. Mochiki, K. Hasegawa and S. Namatame, "Amorphous Silicon Position-Sensitive Detector," *Nucl. Instr. and Meth.* vol. A273, pp. 640-644, 1988.

[6] H. Ito, S. Matsubara, T. Takahashi, T. Shimada and H. Takeuchi, "Integrated Radiation Detectors with a-Si Photodiodes on Ceramic Scintillators," *Jpn. J. Appl. Phys.* vol.28, pp. L1476-L1479, 1989.

[7] R.A. Street, S. Nelson, L. Antonuk and V.Perez-Mendez, "Amorphous Silicon Sensor Arrays for Radiation Imaging," to be published in the Proceedings of the MRS Spring Meeting, San Francisco, CA, Apr. 16-21, 1990.

[8] L.E. Antonuk, J. Yorkston, J. Boudry, M.J. Longo, J. Jimenez and R.A. Street, "Development of Hydrogenated Amorphous Silicon Sensors for High Energy Photon Radiotherapy Imaging," *IEEE Trans. Nucl. Sci*, vol. NS-37, pp. 165-170, 1990.

[9] C.W. Bates, Electrons and Protons, "Scintillation Processes in Thin Films of CsI(Na) and CsI(Tl) due to Low Energy X-rays, Electrons and Protons," *Adv. Electron Physics*, vol. 28A, pp. 451-459, 1968.

[10] A.L.N. Stevels and A.D.M. Schrama de Pauw, "Vapor-Deposited CsI:Na Layers, I. Morphologic and Crystallographic Properties," *Philips Res. Repts* vol. 29, pp. 340-352, 1974.

[11] S. Kubota, S. Sakuragi, S. Hashimoto and J. Ruan, "A New Scintillation Material: Pure CsI with 10ns Decay Time," *Nucl. Instr. and Meth.* vol. A268, pp. 275-277, 1988.
[12] I. Holl, E. Lorenz and G. Mageras, "A measurement of the Light Yield of Some Common Inorganic Scintillators," *IEEE Trans. Nucl. Sci.* vol. NS-35, pp. 105-109, 1988.
[13] Hamamatsu Photonics K.K., 314-5 Shimokanzo, Toyooka-mura, Iwata-gun, Shizuoka-ken, 438-01, Japan. Photomultiplier tubes catalogue, December 1986 and Photodiodes catalogue, March 1986.
[14] P. Schotanus, R. Kamermans and P. Dorebos, "Scintillation Characteristics of Pure and Tl-doped CsI Crystals," *IEEE Trans. Nucl. Sci*, vol. NS-37, pp. 177-182, 1990.
[15] R.D. Giauque, F.S. Goulding, J.M. Jaklevic and R.H. Pehl, "Trace Element Determination with Semiconductor X-ray Spectrometers," *Analytical Chemistry*, vol.45 pp. 671-681, 1973.
[16] M. Kunii, K. Hasegawa, H. Oka, Y. Nakazawa, T. Takeshita and H. Kurihara, "Performance of a High-Resolution Contact-Type Linear Image Sensor with a-Si:H/a-SiC:H Heterojunction Photodiodes," *IEEE Trans. Electron Devices*, vol. ED-36, pp. 2877-2881, 1989.
[17] A.L.N. Stevels and A.D.M. Schrama de Pauw, "Vapor-Deposited CsI:Na Layers, II. Screens for Application in X-Ray Imaging Devices," *Philips Res. Repts* vol. 29, pp. 353-362, 1974.
[18] M. Kobayashi, S. Sakuragi, "Radiation damage of CsI(Tl) crystals above 10^3 rad," *Nucl. Instr. Meth.*, vol. A254, pp. 275-280, 1987.
[19] M.J. Berger, S.M. Seltzer, S.E. Chappell, J.C. Humphreys and J.W. Mots, "Response of Silicon Detectors to Monoenergetic Electrons with Energies between 0.15 and 5.0 MeV," *Nucl. Instr. and Meth.* vol. 69, pp. 181-193, 1969.
[20] T. Takahashi, H. Itoh, T. Shimada and H. Takeuchi, "Design of Integrated Radiation Detectors with a-Si Photodiodes on Ceramic Scintillators for use on X-Ray Computed Tomography," *IEEE Trans. Nucl. Sci*, vol. NS-37, pp.1478-1482, 1990.

APPENDIX ANALYSIS OF PREAMPLIFIER OUTPUT FOR SCINTILLATION LIGHT DETECTION

A scintillator may have multiple scintillation components with different decay constants, each of which corresponds to a particular carrier transition between energy levels. It is often sufficient, however, to treat the scintillation yield as a function of time as a single exponential decay with a characteristic time τ, namely, $Y(t) = Y_0 \exp(-t/\tau)$. We expect that the decay constants of CsI(Tl) and the Hitachi scintillator are comparable with the minimum setting of our X-ray pulse (T_0 = 1-2 μs), whereas, the RC decay constant of our charge-sensitive preamplifier (RC = 1 ms) is comparable to the decay constant of Lanex. Since different assumptions will be made in the analysis, these are treated separately.

A. $\tau \approx T_o << RC$ (CsI(Tl) and the Hitachi scintillator)

The RC discharge of the charge stored in the feedback capacitor of a charge-sensitive preamplifier can be neglected for $\tau << RC$. But the X-ray generation cannot be regarded as instantaneous.

X-ray pulse of duration Δt_o at $t = t_o$ ($0 \le t \le T_o$) yields scintillation light expressed as

$$Y_o \exp\left(\frac{t-t_o}{\tau}\right)\Delta t_o \qquad \text{(A1)}$$

This light creates charge in the external circuit $\Delta Q(t,t_0)$ given by,

$$\Delta Q(t,t_o) = A\int_{t_o}^{t} Y_o \exp\left(\frac{t'-t_o}{\tau}\right) dt'\Delta t_o \qquad \text{(A2)}$$

where, A is the factor involving the light collection and quantum efficiencies.
The total charge created by the X-ray pulse of duration T_0 is expressed as,

$$Q(t) = \int_0^t \Delta Q(t,t_o)\, dt_o \qquad \text{for } 0 \le t \le T_o \qquad \text{(A3)}$$

$$Q(t) = \int_0^{T_o} \Delta Q(t,t_o)\, dt_o \qquad \text{for } T_o \le t \qquad \text{(A4)}$$

These integrals are performed to give the following results.

$$Q(t) = Y_o\tau^2\left\{\frac{t}{\tau} - 1 + \exp\left(\frac{t}{\tau}\right)\right\} \qquad \text{for } 0 \le t \le T_o \qquad \text{(A5)}$$

$$Q(t) = Y_o\tau^2\left\{\frac{T_o}{\tau} - \exp\left(\frac{t}{\tau}\right)\left[\exp\left(\frac{T_o}{\tau}\right) - 1\right]\right\} \qquad \text{for } T_o \le t \qquad \text{(A6)}$$

The total charge observed at infinite time is given by,

$$Q_o = Y_o\,\tau\,T_o \qquad \text{(A7)}$$

Dimensionless expression for the preamplifier output is obtained by dividing Q(t) by Q_o.

B. $T_o << \tau \approx RC$ (Lanex)

In this case, the X-ray generation is assumed as instantaneous but the RC decay of the charge stored in the feedback capacitor cannot be neglected. The preamplifier output is given by the scintillation decay function $Y(t)=Y_o\exp(-t/\tau)$ convolved by the response function of the charge-sensitive preamplifier exp(-t/RC), namely,

$$Q(t) = \int_0^t Y_o \exp\left(-\frac{t_o}{\tau}\right) \exp\left(-\frac{t-t_o}{RC}\right) dt_o \qquad \text{(A8)}$$

Therefore,

$$Q(t) = Y_o\tau'\left[\exp\left(\frac{t}{RC}\right) - \exp\left(\frac{t}{\tau}\right)\right] \qquad \text{(A9)}$$

where,

$$\frac{1}{\tau'} = \frac{1}{\tau} - \frac{1}{RC} \qquad \text{(A10)}$$

It should be noted that eq.(A9) becomes a simple exponential form with a decay constant RC in the limit of $\tau << RC$. This is the case for the CsI(Tl) layer with τ = 1 μs and RC approximately 1 ms.

C. Curve fitting of the measured output

First, the wave forms in Fig.5 were normalized against their asymptotic values to give dimensionless output forms and their initial portions during the X-ray pulse ($0 \le t \le T_o$) were

fitted with the theoretical expression. The decay constant τ is the only fitting parameter used and results with three different τ are plotted in the Fig.A1 for the two scintillators. The best fit is given by τ=1.1 μs for the CsI(Tl) and τ=3.5 μs for the Hitachi scintillator, respectively. These values agree well with published data.

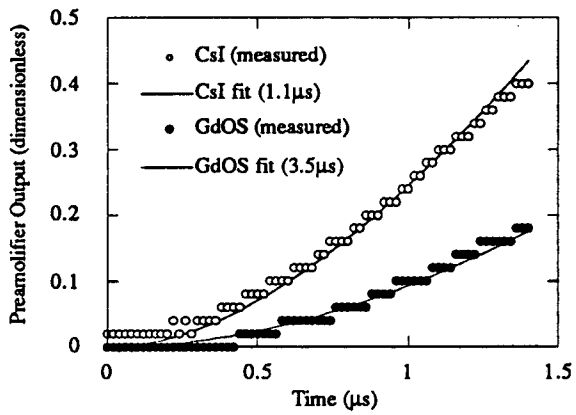

Fig.A1 Dimensionless preamplifier output fitted with the theoretical expression.

Second, the Lanex data were analyzed. Fitting the exponential tail of the CsI(Tl) signal gives the RC decay constant of 1.06 ms. The Lanex signal in Fig.6 can be fit by eq.(A9) using τ as the only fitting parameter as shown in Fig.A2.

Since the wave form is well described by eq.(A9), the peak value (t_{max}, Q_{max}) can be used to calculate τ for Lanex. The expression for these are given by,

$$\tau = RC \exp\left(\frac{t_{max}}{\tau'}\right) \tag{A11}$$

$$Q_{max} = Y_o \tau \left(\frac{\tau}{RC}\right)^{\frac{\tau'}{RC}} \tag{A12}$$

From the peak value t_{max} of 0.700 ms for Lanex, the decay constant of 0.48 ms is obtained by solving eq.(A11) graphically.

The total light yield is given by

$$\int_0^\infty Y_o \exp\left(-\frac{t}{\tau}\right) dt = Y_o \tau \tag{A13}$$

The ratio of the total light yield of CsI(Tl) to that of Lanex is calculated by eq.(A12) and eq.(A13) from the peak values Q_{max} of both wave forms. This ratio is 1.19.

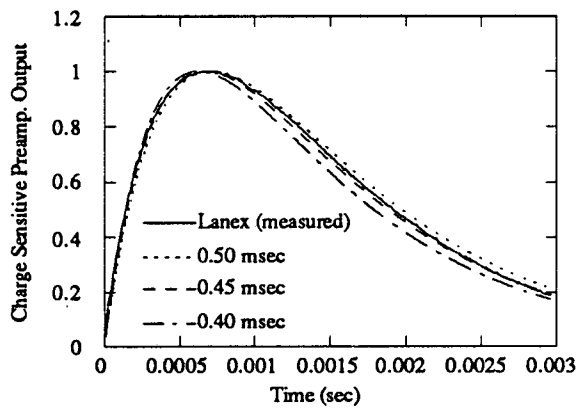

Fig.A2 Fitting the Lanex signal by the analytical expression for the preamplifier output.

LAWRENCE BERKELEY LABORATORY
UNIVERSITY OF CALIFORNIA
INFORMATION RESOURCES DEPARTMENT
BERKELEY, CALIFORNIA 94720